On the Performance of Orthogonal Space-Time Block Codes for Spatially and Temporally Correlated Wireless Channels

Larry T. Younkins
Johns Hopkins University
Applied Physics Laboratory,
Laurel, MD 20723, USA
Email: larry.younkins@jhuapl.edu

Weifeng Su
Department of ECE
University of Maryland,
College Park, MD 20742, USA
Email: weifeng@eng.umd.edu

K. J. Ray Liu
Department of ECE
University of Maryland,
College Park, MD 20742, USA
Email: kjrliu@eng.umd.edu

Abstract—**Monte Carlo simulations are used to determine the performance of several orthogonal space-time block codes for wireless channels that exhibit both temporal and spatial correlation. A channel model is employed that specifies the spatial distribution of the channel scatterers and is based upon recent measurements. A significant degradation in the performance of the space-time codes is observed for cases where the scatterers are located in close proximity to the mobile and fractional wavelength antenna spacing is used at the transmitter. The conditions under which the channel transmission paths may be assumed to be independent are quantified in terms of the scattering radius about the mobile and transmit antenna spacing.**

I. Introduction

Wireless systems employing multiple transmit and receive antennas have the potential for tremendous gains in channel capacity through exploitation of independent transmission paths due to scattering. Diversity combining techniques have been used at the base station receiver for some time and these approaches are well understood [1],[2]. Achieving transmit diversity through the use of space-time coding techniques at the base station is a recent innovation motivated by the need for higher throughput in the wireless channel. A simple two-branch transmit diversity scheme was first proposed by Alamouti [3]. It was demonstrated that this scheme provides the same diversity order as a wireless system employing a single transmit antenna and two receive antennas and utilizing maximal-ratio combining (i.e. classical receive diversity). The bit-error-rate (BER) performance of the proposed scheme was evaluated assuming that the path from each transmit antenna to each receive antenna experiences mutually uncorrelated Rayleigh amplitude fading. Tarokh et al. [4] proposed additional space-time block codes utilizing three and four transmit antennas. These codes are based upon complex-valued orthogonal designs [5] and have the feature that only linear processing is required at the receiver for decoding. The transmission model used in this work assumed that the path gains are independent complex Gaussian random variables. Further, it was assumed that the path gains are constant over the space-time code frame length and vary independently from frame to frame.

The majority of the research to date on space-time coding techniques has employed the assumption of independent transmission paths without regard for the conditions under which this assumption is justified. The degree of correlation between channel transmission paths depends significantly on the scattering environment and on the antenna separation at the transmitter and receiver. For example, if the majority of the channel scatterers are located in close proximity to the mobile then the transmission paths will be highly correlated unless the transmit antennas are sufficiently separated in space. Early research that characterized the spatial and temporal characteristics of the mobile radio channel was performed by Jakes [1] and Clarke [7]. In these works a simple geometric scattering model was employed that places scatterers uniformly on a circular ring a fixed distance from the mobile. More recently, Chen et al. [8] extended this 'circular ring' scatterer model to include multiple antennas at the base station, a single antenna at the mobile and Doppler effects due to motion of the mobile. Shiu et al. [9] investigated the effects of fading correlation on the capacity of multiple-antenna wireless systems by employing the Jakes model to multiple antennas at the base station as well as the mobile. However, Doppler effects due to mobile motion were not considered.

A recent measurement campaign conducted by Pedersen et al. [11],[12],[13] characterized the temporal and azimuth dispersion of multipath in urban wireless environments. Janaswamy [14] determined that these measurements were consistent with a two-dimensional Gaussian density model for the scatterer locations surrounding the mobile receiver. In the work presented here we quantify the performance of space-time coding techniques for a scattering model based upon a two-dimensional Gaussian density. A linear model is employed for the mobile motion and the results include the effects of Doppler.

II. Signal Model

Consider a wireless system employing N_T transmit antennas and N_R receive antennas. The signal received at the q^{th}

0-7803-8255-2/04/$20.00 ©2004 IEEE.

antenna at time t is

$$y_q(t) = \sum_{p=1}^{N_T} h_{p,q}(t) c_p(t) + \eta_q(t) \quad (1)$$

where $\eta_q(t)$ is noise and is assumed to be independent zero-mean complex Gaussian with variance $N_T/(2\,SNR)$ per complex dimension with SNR denoting the signal-to-noise ratio. The quantity $h_{p,q}(t)$ in Equation 1 denotes the complex path gain between the p^{th} transmit antenna and the q^{th} receive antenna at time t. The next section presents the details of the channel model and a expression for the complex path gain. The quantity $c_p(t)$ denotes the space-time code symbol transmitted by the p^{th} antenna at time t. The space-time codes are normalized such that the average energy over all codes is unity. Each code is described by a $T \times N_T$ matrix with the columns corresponding to the space dimension and the rows corresponding to the time dimension. Each entry in the matrix consists of linear combinations of the complex-valued signal constellation variables $x_1, x_2, \ldots, x_k$. These variables are determined by the type of modulation employed (e.g. M-QAM, M-PSK, etc.) and the specific data to be encoded. The space-time code symbol $c_p(t)$ is chosen as the entry in the code matrix corresponding to the p^{th} column and t^{th} row. Three space-time block codes are investigated in the work presented here [4]. The code G_2 is defined by

$$G_2(x_1, x_2) = \begin{pmatrix} x_1 & x_2 \\ -x_2^* & x_1^* \end{pmatrix} \quad (2)$$

Clearly, the rate of the G2 code is 1. This code was first proposed by Alamouti [3] for wireless systems employing $N_T = 2$ transmit antennas. Two codes with rate 3/4 are also employed in the simulation results presented here. They are

$$H_3(x_1, x_2, x_3) = \begin{pmatrix} x_1 & x_2 & \frac{x_3}{\sqrt{2}} \\ -x_2^* & x_1^* & \frac{x_3}{\sqrt{2}} \\ \frac{x_3^*}{\sqrt{2}} & \frac{x_3^*}{\sqrt{2}} & \frac{(-x_1 - x_1^* + x_2 - x_2^*)}{2} \\ \frac{x_3^*}{\sqrt{2}} & -\frac{x_3^*}{\sqrt{2}} & \frac{(x_2 + x_2^* + x_1 - x_1^*)}{2} \end{pmatrix} \quad (3)$$

and

$$H_4(x_1, x_2, x_3) = \quad (4)$$
$$\begin{pmatrix} x_1 & x_2 & \frac{x_3}{\sqrt{2}} & \frac{x_3}{\sqrt{2}} \\ -x_2^* & x_1^* & \frac{x_3}{\sqrt{2}} & -\frac{x_3}{\sqrt{2}} \\ \frac{x_3^*}{\sqrt{2}} & \frac{x_3^*}{\sqrt{2}} & \frac{(-x_1 - x_1^* + x_2 - x_2^*)}{2} & \frac{(-x_2 - x_2^* + x_1 - x_1^*)}{2} \\ \frac{x_3^*}{\sqrt{2}} & -\frac{x_3^*}{\sqrt{2}} & \frac{(x_2 + x_2^* + x_1 - x_1^*)}{2} & -\frac{(x_1 + x_1^* + x_2 - x_2^*)}{2} \end{pmatrix}$$

Codes that are equivalent to these two designs and possess a somewhat simpler form have been found. See [6] for details and additional references. A key feature of the codes G_2, H_3 and H_4 is that only linear processing is required for decoding.

III. Channel Model

This section describes the channel model employed for the Monte Carlo simulations presented here. Consider the path gain associated with the signal received at the q^{th} array element of the antenna at the mobile and transmitted from the p^{th} array element at the base station. It consists of contributions from M discrete scatterers with each scatterer characterized by its amplitude A_m, phase ψ_m and spatial location $\vec{x}_m$. All scatterers are assumed to be coplanar with the mobile and base station. The spatial locations of the array phase centers for the mobile and base are $\vec{x}_{mobile}$ and $\vec{x}_{base}$, respectively. Assuming a plane wave with frequency f_c is transmitted by the base, the expression for the complex path gain $h_{p,q}(t)$ is:

$$h_{p,q}(t) = \sum_{m=0}^{M-1} A_m \exp(j\psi_m) \exp\left[j2\pi f_c(-\tau_m(t))\right] \quad (5)$$
$$\times \exp\left[+j\vec{k}_{mobile}^{m} \cdot \vec{x}_{mobile}^{p} + j\vec{k}_{base}^{m} \cdot \vec{x}_{base}^{q}\right]$$

In the previous expression $\tau_m(t)$ denotes the path delay associated with the m^{th} scatterer and

$$\vec{k}_{mobile}^{m} = k(\cos\theta_m, sin\theta_m, 0) \quad (6)$$

$$\vec{k}_{base}^{m} = k(\cos\phi_m, sin\phi_m, 0) \quad (7)$$

$k = 2\pi/\lambda$ with λ the transmitted wavelength. The angle θ_m corresponds to the angle of arrival at the mobile (array phase center) associated with the signal re-radiated from the m^{th} scatterer and the angle ϕ_m corresponds to the angle of departure of the signal transmitted from the base (array phase center). In order to specify the path delay associated with the m^{th} scatterer, $\tau_m(t)$, some assumptions about the motion of the mobile must be made. In what follows we assume a linear motion model. Specifically, the spatial location of the mobile as a function of time is given by

$$\vec{x}_{mobile}(t) = \vec{x}_{mobile}^{0} + \vec{v}t \quad (8)$$

with $\vec{x}_{mobile}^{0}$ denoting the initial location of the mobile and $\vec{v} = |\vec{v}|\cos(\gamma)$ denoting the velocity vector. The quantity $|\vec{v}|$ is the magnitude of velocity vector and γ is the angle the vector makes with the x-axis of the coordinate system. Using this model, the expression for the path delay is

$$\tau_m(t) = \frac{|\vec{x}_{base} - \vec{x}_m| + |\vec{x}_m - \vec{x}_{mobile}|}{c} \quad (9)$$
$$= \frac{|\vec{x}_{base} - \vec{x}_m| + |\vec{x}_m - (\vec{x}_{mobile}^{0} + \vec{v}t)|}{c}$$

where c denotes the speed of light and $|\vec{x}|$ denotes the norm of the vector $\vec{x}$.

The amplitude A_m and phase ψ_m associated with the m^{th} scatterer depend on the physical characteristics of the scatterer itself [10] and are in general unknown. For the results presented here it is assumed that the scatterer amplitude $A_m = A$ for all m and the scatterer phase ψ_m is uniformly distributed on $(-\pi, \pi)$ and independent for each m.

A key aspect of the channel model is the probability distribution of the M scatterer locations $\vec{x}_m$. Given $\vec{x}_m$, the mobile parameters ($\vec{x}_{mobile}^{0}$ and $\vec{v}$) and the locations of the transmit and receive array phase centers, $\vec{x}_{base}$ and $\vec{x}_{mobile}$, respectively, the path delay $\tau_m(t)$, angle of arrival θ_m and angle of departure ϕ_m associated with the m^{th} scatterer are completely determined. A recent measurement campaign

conducted by Pedersen et al. [11],[12],[13] characterized the temporal and azimuth dispersion of multipath in urban wireless environments. The study found that the power azimuth spectrum was accurately modeled using a truncated Laplacian function and power delay spectrum was well-approximated by a negative-exponential function. Recent work by Janaswamy [14] concluded that the measurements reported by Pedersen et al. were consistent with a two-dimensional Gaussian density model for the scatterer locations surrounding the mobile receiver. Expressions were derived for the root-mean-square (RMS) angular spread and RMS delay spread as a function of the distance D between the mobile and the base and the Gaussian spread parameter σ_R (denoted by σ_s in [14]). The parameter σ_R specifies a radius about the mobile for which approximately 68 percent of the scatterers are contained. Similarly, the value $2\sigma_R$ specifies a radius for which roughly 95 percent of the scatterers are contained. The two-dimensional Gaussian scatterer density model was used for the simulation results presented here.

IV. Simulation Results

For the Monte Carlo simulations M=50 discrete scatterer locations were generated about the mobile using the two-dimensional Gaussian scatterer model. Values considered for the parameter σ_R were σ_R=10, 20, 50, 100, 200, 500m and the separation between the mobile and the base was fixed at D=1000m. For reference, Janaswamy determined the best fit parameters for the measurements of Pedersen et al. to be D/σ_R=9.62 yielding σ_R=104m for D=1000m. The magnitude of the mobile velocity vector was chosen to be $|\vec{v}|$=100km/hr resulting in a maximum Doppler shift of 78.7Hz for a carrier frequency of f_c=850MHz. The symbol rate for all modulation schemes was 24000symbols/sec resulting in a data-to-fading ratio of approximately 300:1. We call this case 'slow fading'. For a fixed value of σ_R and signal-to-noise ratio the symbol error probability was calculated by averaging the symbol error over 10000 space-time symbols transmitted and 100 channel realizations.

For the G_2 code the input symbols to the space-time encoder were selected from a $8PSK$ constellation and for the H_3 and H_4 codes the input symbols were selected from a $16QAM$ constellation. Since the rate of the space-time code G_2 is 1 and the rate of both codes H_3 and H_4 is 3/4, the spectral efficiency for all space-time codes investigated was 3 bits/sec/Hz.

Figure 1 shows the simulation results for the G_2 $8PSK$ code with $\lambda/2$ element spacing at the base antenna array and N_T=2, N_R=1. Also shown for reference is the symbol error probability for $8PSK$ modulation in Rayleigh fading (i.e., no space-time coding). Note that for small values of the parameter σ_R, corresponding to scatterers in close proximity to the mobile, significant degradation in the performance of the space-time code is observed. For example, the SNR required to achieve a symbol error probability of 10^{-4} for an uncorrelated channel is approximately 29dB but increases to more than 40dB for σ_R=10m. The latter case corresponds closely to the result for no space-time coding. From the figure it is also observed that the symbol error probability for the σ_R=500m case is essentially the same as that for the uncorrelated channel. Figure 2 shows the simulation results for the G_2 $8PSK$ code with 5λ element spacing at the base antenna array. Considerable improvement in the performance of the space-time code is observed for this case, particularly for small values of the parameter σ_R. It was found that approximately 30λ spacing of the base antennas was required to achieve performance within 0.5dB of that observed for the uncorrelated channel at 10^{-4} symbol error probability for σ_R=10m.

Figure 3 shows the simulation results for the H_3 $16QAM$ code with $\lambda/2$ element spacing at the transmitter and N_T=3, N_R=1. For this case the SNR required to achieve a symbol error probability of 10^{-4} is approximately 27dB for the uncorrelated channel, achieving a gain of 2dB over the G_2 $8PSK$ code. However, for σ_R=10m the results correspond closely to the case of no space-time coding. Figure 4 shows the results for the H_3 $16QAM$ code with 5λ element spacing at the transmitter. For this case the symbol error probabilities for σ_R=50, 100, 200, 500m are essentially identical to that for the uncorrelated channel. It was found that approximately $\tilde{4}0\lambda$ spacing of the base antennas was required to achieve performance within 0.5dB of that observed for the uncorrelated channel at 10^{-4} symbol error probability for σ_R=10m.

Figures 5 and 6 show the results for the H_4 $16QAM$ code with $\lambda/2$ and 5λ element spacing at the transmitter, respectively. For this case, to achieve a symbol error probability of 10^{-4} for the uncorrelated channel requires approximately 25dB SNR, a gain of 4dB over the G_2 $8PSK$ code and 2dB over H_3 $16QAM$ code. However, for small values of the parameter σ_R severe degradation in the performance of the space-time code is observed, particularly for $\lambda/2$ element spacing.

V. Conclusions

Monte Carlo simulations were used to determine the performance of several orthogonal space-time block codes using a two-dimensional Gaussian scatterer model. Codes employing 2, 3 and 4 transmit antennas, a single receive antenna, and with a spectral efficiency of 3bits/s/Hz were investigated. A significant degradation in performance was observed for cases in which the scatterers were located in close proximity to the mobile and fractional wavelength spacing was employed at the transmitter. Increasing the transmit antenna spacing mitigates this effect to a certain extent and the antenna spacing required in order to achieve performance comparable to the uncorrelated channel was quantified.

References

[1] W.C. Jakes, *Microwave Mobile Communications*, IEEE-Press, 1974.

[2] J. Winters, "Optimum Combining in Digital Mobile Radio with Cochannel Interference," *IEEE Journal on Selected Areas in Communications*, Vol. SAC-2, No. 4, pp. 528-539, July 1984.

[3] S. Alamouti, "A Simple Transmit Diversity Technique for Wireless Communications," *IEEE Journal on Selected Areas in Communications*, Vol. 16, No. 8, October 1998.

[4] V. Tarokh et al., "Space-Time Block Coding for Wireless Communications: Performance Results," *IEEE Journal on Selected Areas in Communications*, Vol. 17, No. 3, March 1999.

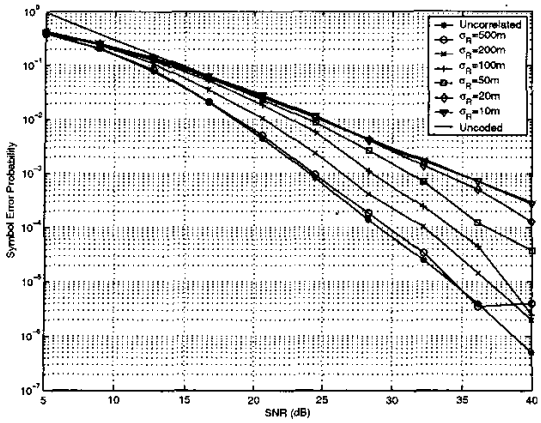

Fig. 1. G_2 $8PSK$ code, Gaussian scatterer density model, slow fading, N_T=2, $\lambda/2$ element spacing, N_R=1. Symbol error probability versus per symbol signal-to-noise ratio.

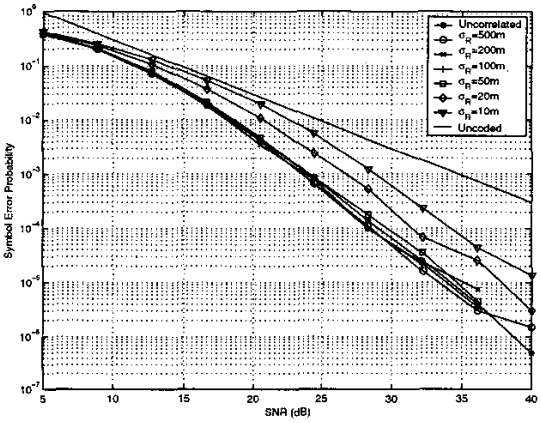

Fig. 2. G_2 $8PSK$ code, Gaussian scatterer density model, slow fading, N_T=2, 5λ element spacing, N_R=1. Symbol error probability versus per symbol signal-to-noise ratio.

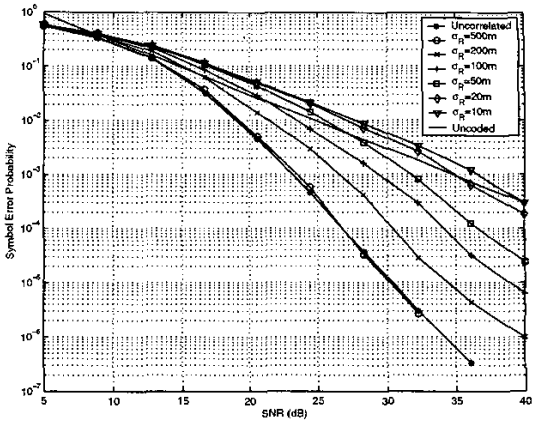

Fig. 3. H_3 $16QAM$ code, Gaussian scatterer density model, slow fading, N_T=3, $\lambda/2$ element spacing, N_R=1. Symbol error probability versus per symbol signal-to-noise ratio.

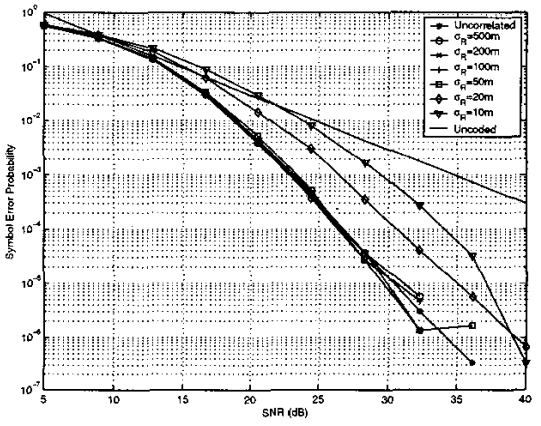

Fig. 4. H_3 $16QAM$ code, Gaussian scatterer density model, slow fading, N_T=3, 5λ element spacing, N_R=1. Symbol error probability versus per symbol signal-to-noise ratio.

[5] V. Tarkokh et al., "Space-Time Block Codes from Orthogonal Designs," *IEEE Transactions on Information Theory*, Vol. 45, No. 5, July 1999.

[6] W. Su and X.-G. Xia, "On Space-Time Block Codes from Complex Orthogonal Designs," *Wireless Personal Communications*, Vol. 25, No. 1, pp.1-26,2003.

[7] R.H. Clarke, "A Statistical Theory of Mobile-Radio Reception," *Bell System Technical Journal*, pp.957-1000, July-Aug. 1968.

[8] T.A. Chen et al. "A Space-Time Model for Frequency Nonselective Rayleigh Fading Channels with Applications to Space-Time Modems," *IEEE Journal on Selected Areas in Communications*, Vol. 18, No. 7, July 2000.

[9] D.S. Shiu et al. "Fading Correlation and Its Effect on the Capacity of Multielement Antenna Systems," *IEEE Transactions on Communications*, Vol. 48, No. 3, March 2000.

[10] Constantine A. Balanis, *Antenna Theory, Analysis and Design*, J. Wiley & Sons, 1997.

[11] K. Pedersen, P. Mognesen, and B. Fleury, "A Stochastic Model of the Temporal and Azimuthal Dispersion Seen at the Base Station in Outdoor Propagation Environments," *IEEE Transactions on Vehicular Technology*, Vol. 49, No. 2, pp. 437-447, Mar. 2000.

[12] K. Pedersen, P. Mognesen, and B. Fleury, "Power Azimuth Spectrum in Outdoor Environments," *Electronics Letters*, Vol. 33, No. 18, pp. 1583-1584, Aug. 1997.

[13] K. Pedersen, P. Mognesen, and B. Fleury, "Spatial Channel Characteristics in Outdoor Environments and their Impact on the BS Antenna System Performance," in *IEEE Vehicular Technology Conf.*, 1998, pp. 719-723.

[14] R. Janaswamy, "Angle and Time of Arrival Statistics for the Gaussian Scatter Density Model," *IEEE Transactions on Wireless Communications*, Vol. 1, No. 3, July 2002.

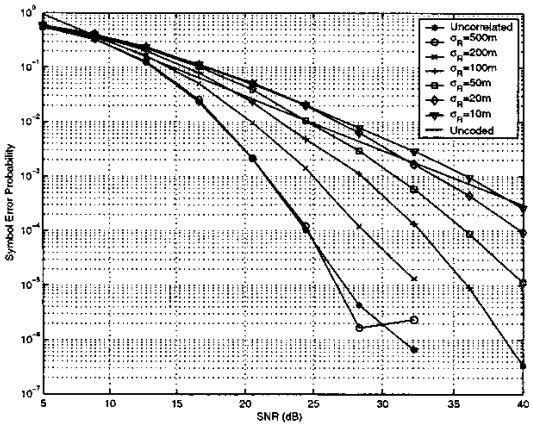

Fig. 5. H_4 $16QAM$ code, Gaussian scatterer density model, slow fading, N_T=4, $\lambda/2$ element spacing, N_R=1. Symbol error probability versus per symbol signal-to-noise ratio.

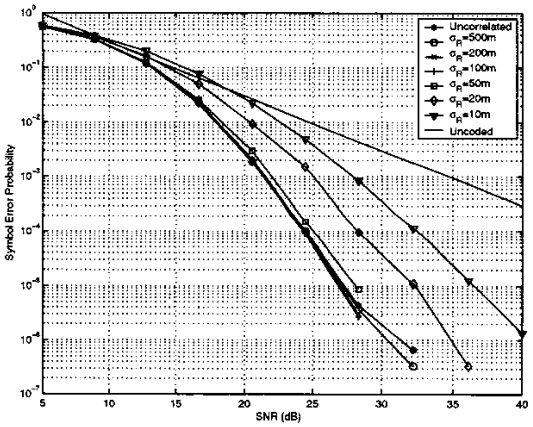

Fig. 6. H_4 $16QAM$ code, Gaussian scatterer density model, slow fading, N_T=4, 5λ element spacing, N_R=1. Symbol error probability versus per symbol signal-to-noise ratio.